

Damage Behavior in Modern automotive High Strength Dual Phase Steels During Uniaxial Tensile Deformation

N. Saeidi¹, F. Ashrafizadeh², B. Niroumand³, F. Barlat⁴

^{1,2,3} Department of Materials Engineering, Isfahan University of Technology, Isfahan 84156-83111, Iran

⁴ Materials Mechanics Laboratory (MML), Graduate Institute of Ferrous Technology (GIFT), Pohang University of Science and Technology (POSTECH), South Korea

Abstract

In the present research, damage mechanisms during room temperature uniaxial tensile testing of two different modern high strength dual phase steels, DP780 and DP980, were studied. Detailed microstructural characterization of the strained and sectioned samples was performed by scanning electron microscopy (SEM). The results revealed that interface decohesion, especially at the triple junctions of ferrite-ferrite-martensite, was the most probable mechanism for void nucleation. Also, it was found that ductile fracture in these steels was nucleation controlled such that just before ductile fracture incidence, a high density of voids would nucleate or a sudden accelerated void nucleation could happen. Microscopic observations as well as statistical analysis confirmed this phenomenon. Moreover, damage analysis suggested that the void nucleation rate was higher in DP980 than DP780 steel. It seemed to be highly influenced by the morphology and distribution of martensite particles within the ferrite matrix.

Keywords: Dual phase steel; Damage mechanism; Interface strength.

1. Introduction

Ductile fracture of metals mainly involves three processes of void nucleation, growth, and coalescence¹⁾. In order to control these phenomena and enhance the resistance of materials to fracture, a detailed understanding of fracture mechanism is required. While the subject is well established for various ductile alloys, in the new important field of modern high strength dual phase (DP) steels, especially in giant automobile industry, few researches have been reported. It has been shown that in DP steels, the second hard phase particles act as void nucleation sites²⁻⁴⁾. However, nucleated cavities in DP steels, due to the constraining effect of martensite particles, cannot grow in transverse direction⁵⁾. Erdogan⁶⁾ studied the effect of microstructural parameters such as grain size and martensite content on the ductile fracture of DP steels. This research showed that in both fine and coarse grain microstructures, the formation of micro voids at martensite particles, inclusions, and martensite-ferrite interfaces in the necked region was prevalent. Also, it was shown that coarse and interconnected

martensite particles distributed along ferrite grain boundaries were mostly prone to easy cracking, while in fine grain structures, martensite cracking was less frequent. In another work, by analyzing coarse, fine and ultra-fine grained DP steels, Calcagnotto et al.⁷⁾ showed that with decreasing the grain size, due to the lower number of dislocations piled up within ferrite grains and the subsequent lower shear stress acting on martensite particles, the probability of martensite cleavage cracking was decreased such that it was less frequent in ultra-fine steels. Steinbrunner et al.⁸⁾ studied different DP steels and showed that with increasing martensite volume fraction, necking strain was decreased due to the higher amount of void nucleation in the material. Also, they showed that void nucleation was a direct consequence of strain gradient between ferrite and martensite in DP steels. Cingara et al.^{9,10)} have reported that four main mechanisms cause the occurrence of void nucleation in DP600 steels. These include nucleation of voids on cracked martensite particles at low strains and mainly in large particles of martensite, nucleation of voids at martensite/martensite interface at high strains, nucleation of voids on ferrite/martensite interface at all strain levels, which is more obvious at high strains, and nucleation of voids at inclusion, which is rare because of the high quality of commercial DP steels. In accordance with the literature, decohesion of ferrite/martensite interface is the most probable mechanism of voids nucleation which grows mostly perpendicular to the tensile direction, along ferrite grain boundaries,

* Corresponding author

Tel: +98 9131654591

Fax: +98 311 3912752

Email: navidsae@gmail.com

Address: Department of Materials Engineering, Isfahan University of Technology, Isfahan 84156-83111, Iran

1. Ph.D. Student

2. Professor

3. Associate Professor

4. Professor

and can be affected by the size, shape and distribution of the second phase particles as well as the presence of impurities or hydrostatic stress¹¹⁾.

In the present work, ductile damage evolution of two different commercial high strength sheet steels, i.e. DP780 and DP980, has been studied. These two types of steel, which have different martensite particles morphologies and volume fractions, are rather new and their damage behavior has not been studied. The main objective of this study was to evaluate and compare damage performance of DP780 and DP980 steel sheets during room temperature uniaxial tensile test. Damage analysis was performed by the examination of metallographic sections and quantitative fractography of tensile specimens using SEM.

2. Materials and methods

Materials used for this research were DP780 and DP980 sheet steels provided by POSCO Company. Tensile specimens were machined according to ASTM E8 standard, in rolling direction, using electrodischarge machining (EDM) method. The gauge length was 50 mm and tensile tests were carried out at a constant cross head speed of 0.03 mm/s with a servo-hydraulic MTS machine.

Fracture surface of the specimens was analyzed by SEM equipped with an energy dispersive spectrometer (EDS) for microanalysis. The specimens were then sectioned through thickness along the mid-width in longitudinal direction (Figure 1) using Struers cutting machine. In order to measure local strains during deformation, these sectioned specimens were mounted, ground and polished till 4000 grit finish, which was then followed by polishing with one micrometer diamond suspension and etched in 2% Nital solution. Then variation of void features across the length of the specimen was studied by image analysis of SEM micrographs, using Image J software; martensite volume fraction, f_m , in un-deformed material was measured too.

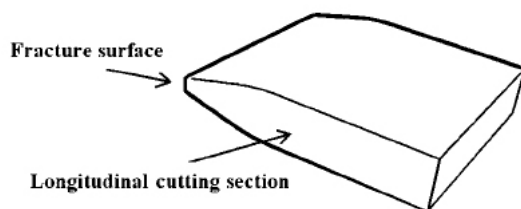


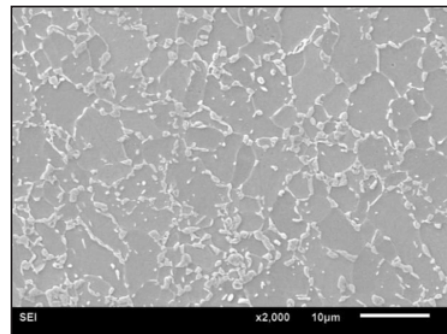
Fig. 1. Schematic illustration of longitudinal sectioned specimens.

3. Results and discussions

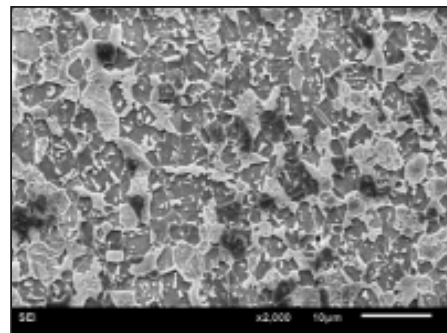
3.1. Microstructures and tensile properties

Figure 2 shows the microstructure of DP steels

studied; in both micrographs, there was a uniform distribution of small martensite particles. In DP780, the particles were more uniform in size with more rounded edges rather than DP980, in which martensite particles included sharp edges and less uniform sizes.



(a)



(b)

Fig. 2. Microstructure of (a) DP780 and (b) DP980 steel.

Important mechanical parameters drawn from uniaxial engineering tensile tests along rolling direction are summarized in Table 1. They include ultimate tensile strength, yield stress, elongation, n and k value in Holloman relationship. As can be seen, DP980 had an ultimate tensile stress of 1034 MPa and an elongation of about 10%, while these values for DP780 were about 893 MPa and 24%, respectively.

Table 1. Room temperature tensile properties of DP780 and DP980 steels.

	σ_y (MPa)	σ_{uts} (MPa)	n	K (MPa)	EI %
DP780	550	893	0.22	1651	24
DP980	820	1034	0.16	1853	10

3.2. Fracture mechanism based on SEM observation

By considering SEM observations of the sectioned specimens, regardless of specimen type, four

mechanisms of void nucleation could be identified. One of these mechanisms was void nucleation by martensite particle cracking, which was evident in few martensite grains at rather low strains (Figure 3). Formation of void at ferrite/martensite interfaces was the other mechanism that occurred nearly at all strains, but it was very significant near the final deformation steps, i.e., just before fracture. Inhomogeneous deformation on a microscopic scale between the soft phase of ferrite and the hard phase of martensite should be accommodated at grain boundaries. Also, microscopic triaxiality, which was due to the differences in strength and morphology between the two constituent phases, caused an increase in the stress applied at the grain boundaries ¹².

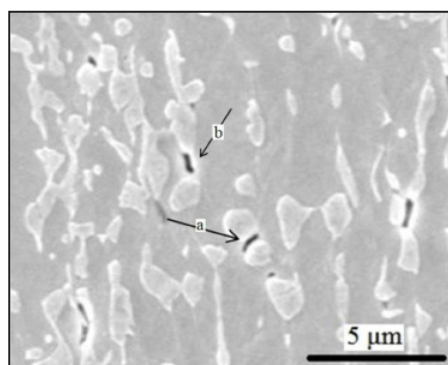


Fig. 3. Void nucleation by martensite cracking (showed by arrow "a") and between martensite particles located at the ferrite grain boundaries, by interface decohesion (showed by arrow "b"). This figure is related to DP780 steel; however, the same behavior was observed in DP980 steel.

So, in large strains, where this accommodation cannot take place, the grain boundary is likely to be damaged by void formation. It seems that under the condition of closely spaced hard particles in the tensile direction, the interaction between plastic fields of particles could be maximized. This interaction can be accentuated in the weak parts of the microstructure, such as triple junctions and grain boundaries. Thus, it can be inferred that void initiation is more affected by particle location rather than particle size. It has been reported ¹³ that network deformation bands developed around hard particles in a soft matrix are strongly dependent on the crystal lattice orientation of the matrix with respect to the particle; this could be the reason why void nucleation does not happen in all similar martensite particles at ferrite grain boundaries. Figure 3 shows the void nucleation at the spacing between those fine martensite particles located at ferrite grain boundaries. A similar behavior was reported by Fisher et al. in spheroidized steel, between ferrite and cementite particles ¹⁴.

The third mechanism (Figure 4) is the formation of voids at Al_2O_3 inclusions, as indicated by EDS analyses, because of inclusion breakage or inclusion/

matrix interface decohesion that provokes the creations of large voids. This kind of void is created at rather low strains and is highly dependent on the inclusion size. It could be due to the incoherency and large mismatch at the inclusion/matrix interfaces. It does not need high stresses to initiate crack/void in these inclusions or at their interfaces. Generally, stress concentration and dislocation pile up around these interfaces cause inclusion fracture or interface decohesion at low strains. On the other hand, it was noticed in this study that these voids did not grow much and there was no coalescence between them.

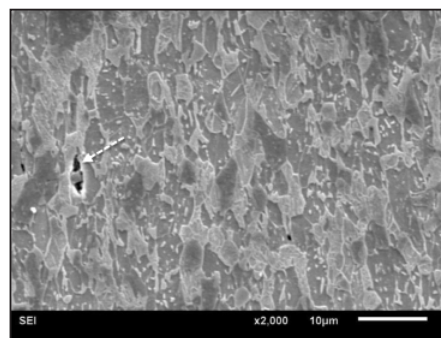


Fig. 4. Formation of voids at inclusions in DP980 steel, indicated by arrow.

The last observed void formation mechanism in the microstructure referred to void formation in the middle of ferrite grains, as can be seen at low strains (Figure 5), at true strain of about 0.1. These voids, circular in shape, were situated within the large ferrite grains. These voids may be formed due to metal contraction during solidification processes. As a whole, the density of these voids is very small in comparison with other types of voids; therefore, they do not seem to be effective in the fracture process of the specimens and so, they can be neglected in fracture analysis.

To summarize, detailed microstructural SEM studies proved that the most probable void formation sites were the closely spaced martensite grains situated at the ferrite grain boundaries; this is in agreement with the observations of Szewczyk and Gurland¹⁵ in a ferrite- 16% martensite DP steel.

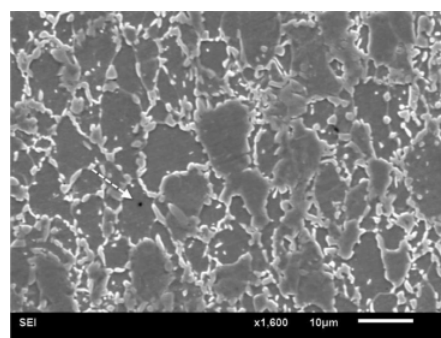
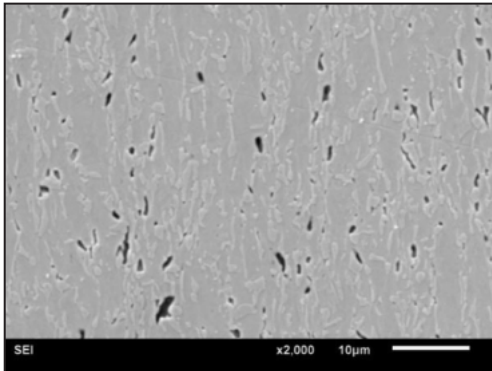
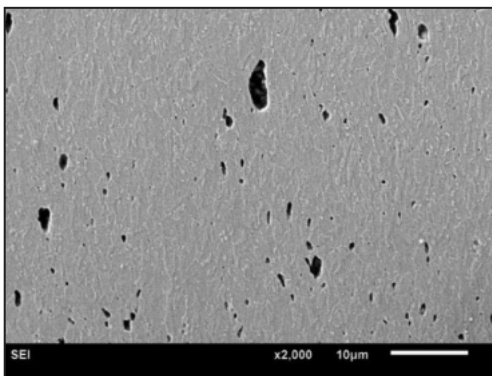


Fig. 5. Void formation in the middle of ferrite grains in DP780 steel, indicated by arrow.

Figure 6 shows the void characteristics behind the fracture surface; this region could be assumed as the critical failure region. It seems that in DP780 specimen, there is the high density of elongated voids in this region while in DP980 specimen, larger voids are the main feature of critical failure condition.



(a)



(b)

Fig. 6. Accelerated void nucleation just before fracture surface for (a) DP780 and (b) DP980 steel.

This behavior can be attributed to the higher strain gradient (Figure 7) due to the higher constraint in DP980 as compared to DP780 steel. It was shown that with increasing martensite volume fraction in DP steels, necking behavior tended to shift from the diffused to localized manner as a result of higher strength and constraint in the material⁸⁾. Diffuse necking was mainly accompanied with extensive post uniform width reduction, while in the localized necking, sample width was approximately unchanged and necking was mostly concentrated in the thickness of the sheet material. Enhanced constraint means a higher triaxiality in the necked region and as Rice and Tracey have shown¹⁾, increasing the triaxiality leads to the acceleration of void growth. Therefore, the higher martensite volume fraction in DP980 steel could be the main reason for the higher triaxiality and the resulting larger voids in the necked area.

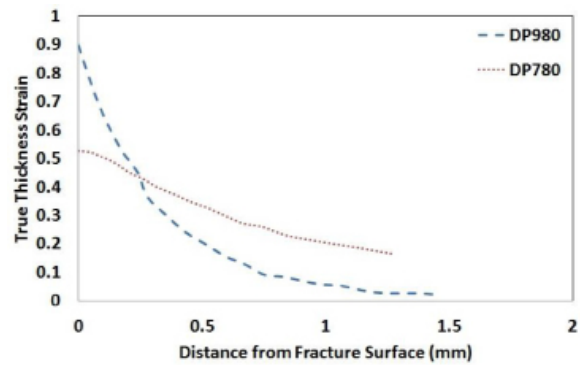
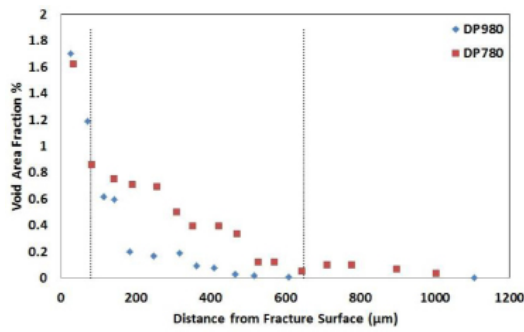


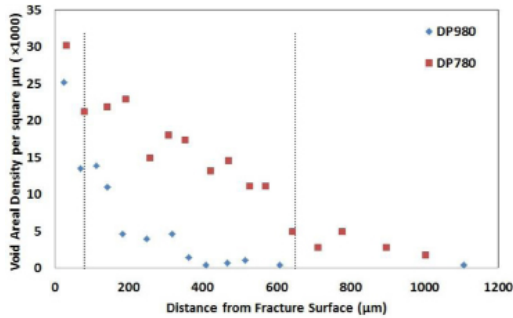
Fig. 7. Strain gradient in longitudinal direction in DP980 and DP780 steels.

Evolution of void area fraction with the distance from fracture surface is shown in Figure 8a. As can be seen, in both steels, before a distance of about 300-600 μm , increment of void area fraction (f_v) with strain had a low rate and it was somewhat monotonic; after that, an accelerated increase of f_v was evident. There was more delay in the accelerated increase of f_v in DP980 steel such that until the distance of about 300 μm from fracture surface, void area fraction did not show any noticeable variation and beyond that, the accelerated increase of f_v could happen; this transient distance was about 500 μm in DP780. The same trend was observable in the evaluation of void areal density (Figure 8b) for which there was a sharp increase in the density of voids in a small distance, about 300 μm for DP980 and 600 μm for DP780 steel. This can be referred to as critical failure region, from the fracture surface. The slope of void areal density variation with distance indicated the void nucleation rate, thereby showing a nucleation rate for DP980 twice higher than DP780 steel. On the other hand, variation of average void area with strain (Figure 8c) showed an approximately fixed rate of void growth within the applied strain range till the final fracture. Overall, it can be inferred that the sharp increase of f_v values in the small distance of fracture surface was more affected by void nucleation rather than void growth. Therefore, in the fracture process, which was mainly nucleation controlled, the voids were mostly nucleated in the ferrite/martensite interfaces by interface decohesion.

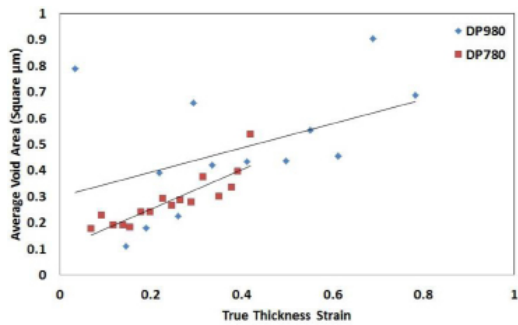
Statistical analysis of voids, void size distribution, just behind the fracture surface, is shown in Figure 9. In both tested steels, most of the voids had a surface area below 0.5 μm^2 , showing very little growth of voids before the final fracture or acceleration of void nucleation in the final steps of deformation. Due to the approximately same value of frequency peak for both steels, it can be concluded that fracture process was mainly influenced by the same mechanism.



(a)



(b)



(c)

Fig.8. Variation of (a) void area fraction, (b) void areal density and (c) void average area versus distance from fracture surface for DP780 and DP980 steel.

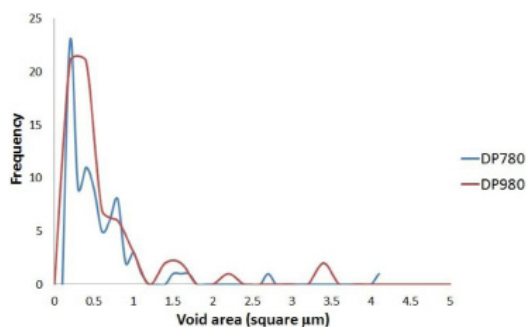


Fig. 9. Frequency of void surface Area distribution in DP780 and DP980 steels, behind the fracture surface.

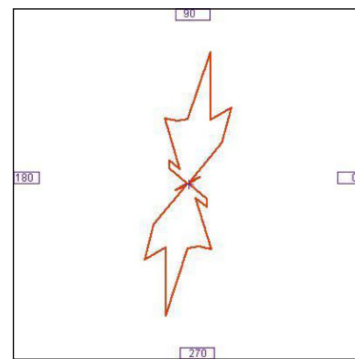
Fisher et al.¹⁴⁾ showed that with decreasing hard particle spacing/particle radius, L/r ratio, the flow stress between hard particles in the matrix was increased. So the probability of void formation was increased; in other words, the void nucleation rate

was increased. The ratio of the hard particles spacing to particle radius in a plane can be obtained by the following relationship¹⁶⁾,

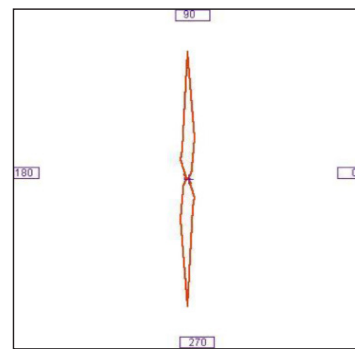
$$\frac{L}{r} = \sqrt{\frac{2\pi}{3f_m}} - \sqrt{\frac{8}{3}} \quad (3)$$

where f_m is the volume fraction of martensite. The value of f_m was obtained to be 17.3% and 40.2% for DP780 and DP980 steels, respectively, and the ratio of L/r was about 1.85 and 0.65, respectively. Therefore, it appears that the observed higher rate of void nucleation in DP980steel is highly affected by the values of L/r ratio.

Orientation of voids just before fracture is shown in Figure 10. It seems that in DP780 steel, voids had an inclined orientation with respect to tensile direction and this difference was about 10°. Distribution of this parameter was mainly in the loading direction, much narrower for DP980 steel which experienced a higher triaxiality and the resulting more void growth (according to what can be inferred from Figure 8 and the results of the next section). These observations showed that void growth due to triaxiality mainly occurred in the loading direction.



(a)



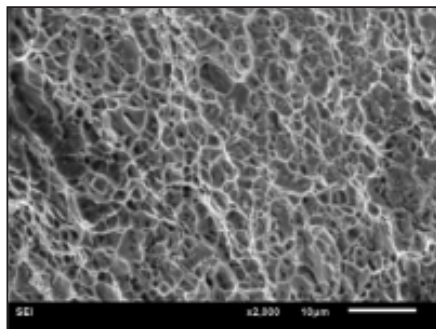
(b)

Fig. 10. Orientation of voids just before fracture, in which degree of 90° is tensile direction, (a) DP780 and (b) DP980 steel.

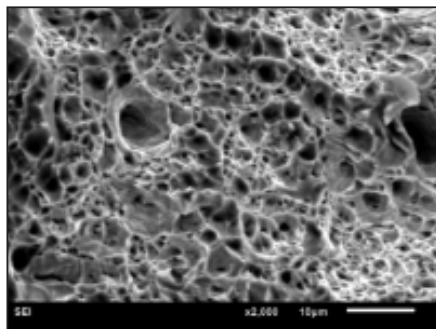
3.3. Fractography analysis

Figure 11 shows SEM micrographs of the fracture surface of DP780 and DP980 steels prepared from the central part of the fracture surface for which plain

strain condition was expected. It is evident that the average dimple size for DP980 was larger than DP780 steel. This is in agreement with the observed larger voids behind the fracture surface (Figure 7 and 9) in DP980 steel. Also, dimples size distribution in DP980 was not as uniform as in DP780 steel, but as a whole, in both steels, most dimples had a low depth, indicating the link-up between the high number density of the neighboring voids.



(a)



(b)

Fig. 11. SEM micrograph of (a) DP780 and (b) DP980 fracture surface.

As the density of dimples per unit area on the fracture surface depends mainly on the number of nucleated voids in the deformed material, if many nucleated voids are present, void growth is limited because of the intersect and link up of the neighboring dimples. So, the final fracture surface appearance consists of many small, shallow dimples. Moreover, the observed high density of fracture surface dimples in both steels was an indication of accelerated void nucleation^{17, 18}, in agreement with the results of section 3.2.

To summarize, it was shown that most of the voids were formed at grain boundaries, where discrete martensite particles were situated. In other words, triple junctions of ferrite-ferrite-martensite were the most preferred sites for void nucleation. Also, by quantitative comparison of martensite particles morphology, the higher void nucleation probability, which was an indication for damage resistance of the material, and the resulting higher void nucleation rate in DP980 steel, was justified.

4. Conclusions

In the present research, two high strength structural steels, i.e. DP780 and DP980 steels, were mechanically tested under room temperature uniaxial tensile test conditions. From the analysis of the microstructures and fractography, the mechanism of damage could be summarized as:

1. Void nucleation mechanism was the same in both DP980 and DP780 sheet steels, and it primarily occurred by the fragmentation or interface decohesion of martensite particles, especially at the triple junctions.
2. Regardless of martensite morphology and volume fraction, both steels showed the same ductile fracture behavior, i.e., fracture was controlled by void nucleation; and it was found that fracture mainly occurred by accelerated void nucleation in the final steps of tensile deformation, where void nucleation rate was higher for DP980 than DP780 steel.
3. It was shown that the observed higher value of void nucleation rate in DP980 steel was highly influenced by martensite particles morphology, i.e., L/r ratio.

References

- [1] J.R. Rice, D.M. Tracey: *J. Mech. Phys. Sol.*, 17(1969), 201.
- [2] K. Kocatepe, M. Cerah, M. Erdogan: *Mater. Des.*, 28(2007), 172.
- [3] M. Erdogan, S. Tekeli: *Mater. Des.*, 23(2002), 597.
- [4] M. Sarwar, E. Ahmad, K. A. Qureshi, T. Manzoor: *Mater. Des.*, 28(2007), 335.
- [5] C. Landron, E. Maire, O. Bouaziz, J. Adrien, L. Lecarme, A. Bareggi: *Acta. Mater.*, 59(2011), 7564.
- [6] M. Erdogan: *J. Mater. Sci.*, 37(2002), 3623.
- [7] M. Calcagnotto, D. Ponge, D. Raabe: *Mater. Sci. Eng. A.*, 527(2010), 7832.
- [8] D.L. Steinbrunner, D.K. Matlock, G. Krauss: *Metall. Trans.*, 19A (1988), 579.
- [9] G. Avramovic-Cingaraa, Y. Ososkova, M.K. Jainb, D. S. Wilkinson: *Mater. Sci. Eng. A.*, 516(2009), 7.
- [10] G. Avramovic-Cingara, C.A.R. Saleh, M.K. Jain, D.S. Wilkinson: *Metall. Mater. Trans. A.*, 40(2009), 3117.
- [11] I.G. Park, A.W. Thompson: *Acta. Metall.*, 36(1988), 1653.
- [12] C. Landron, O. Bouaziz, E. Maire, J. Adrien: *Scripta. Mater.*, 63(2010), 973.
- [13] H.J. Chang, A. Gaubert, M. Fivel, S. Berbenni, O. Bouaziz: *Comput. Mater. Sci.*, 52(2012), 33.
- [14] J.R. Fisher, J. Gurland: *Metal. Sci.*, (1981), 193.
- [15] A.E. Szewczyk, J.A. Gurland: *Metall. Mater. Trans. A.*, 13(1982), 1821.
- [16] A. S. Argon, J. Im, R. Safoglu: *Metall. Mater. Trans. A.*, 6A (1975) 825.
- [17] G. Liu, S. Scudino, R. Li, U. Kühn, J. Sun, J. Eckert: *Mech. Mater.*, 43(2011), 556.
- [18] A. Kumar, S.B. Singh, K.K. Ray: *Mater. Sci. Eng. A.*, 474(2008), 270.